

PAPER • OPEN ACCESS

## First experimental data of the cryogenic safety test facility PICARD

To cite this article: C Heidt *et al* 2017 *IOP Conf. Ser.: Mater. Sci. Eng.* **171** 012044

View the [article online](#) for updates and enhancements.

### Related content

- [Commissioning of the cryogenic safety test facility PICARD](#)  
C Heidt, H Schön, M Stamm et al.
- [Safety studies on vacuum insulated liquid helium cryostats](#)  
C Weber, A Henriques, C Zoller et al.
- [Cryogenic safety in helium cryostats at CERN](#)  
Vittorio Parma and Yann Leclercq

# First experimental data of the cryogenic safety test facility PICARD

C Heidt<sup>1,2</sup>, A Henriques<sup>3</sup>, M Stamm<sup>1</sup> and S Grohmann<sup>1,2</sup>

<sup>1</sup> Karlsruhe Institute of Technology, Institute for Technical Physics,  
Hermann-von-Helmholtz-Platz 1, 76344 Eggenstein-Leopoldshafen, Germany

<sup>2</sup> Karlsruhe Institute of Technology, Institute for Technical Thermodynamics and  
Refrigeration, Kaiserstrasse 12, 76131 Karlsruhe, Germany

<sup>3</sup> European Organization for Nuclear Research (CERN), CH-1211, Geneva 23, Switzerland

E-mail: carolin.heidt@kit.edu, andre.henriques@cern.ch, michael.stamm@kit.edu,  
steffen.grohmann@kit.edu

**Abstract.** The test facility PICARD, which stands for **P**ressure **I**ncrease in **C**ryostats and **A**nalysis of **R**elief **D**evelopments, has been designed and constructed for cryogenic safety experiments. With a cryogenic liquid volume of 100 L, a nominal design pressure of 16 bar(g) and the capacity of measuring helium mass flow rates through safety relief devices up to 4 kg/s, the test facility allows the systematic investigation of hazardous incidents in cryostats under realistic conditions. In the course of experiments, the insulating vacuum is vented with atmospheric air or gaseous nitrogen at ambient temperature under variation of the venting diameter, the thermal insulation, the cryogenic fluid, the liquid level and the set pressure in order to analyze the impact on the heat flux and hence on the process dynamics. A special focus will be on the occurrence and implications of two-phase flow during expansion and on measuring the flow coefficients of safety devices at cryogenic temperatures. This paper describes the commissioning and the general performance of the test facility at liquid helium temperatures. Furthermore, the results of first venting experiments are presented.

**Keywords:** Cryogenics, liquid helium, safety, pressure increase

## 1. Introduction

The pressure relief system of large cryogenic systems, especially liquid helium cryostats, usually requires a staged interaction against overpressure, including a combination of a safety valve and a rupture disc. While the safety valve is often seized for reasonably foreseeable events such as accidental or induced quenches of superconducting components, the rupture disc is dimensioned for catastrophic events like the major loss of insulating vacuum, usually involving a subsequent quench of superconducting magnets. Thus, the bursting pressure of the rupture disc is set to a higher pressure than the opening pressure of the safety valve. [1, 2]

The dimensioning of cryogenic safety relief devices requires detailed knowledge on the processes and process dynamics following hazardous incidents, such as the venting of the insulating vacuum with atmospheric air. However, the established standards and design codes [3–8] are not fully tailored to low temperature cryogenics. For example, the process dynamics are often neglected and the sizing of cryogenic safety relief devices is instead based on few constant (maximum) heat flux data [9–11], yielding potentially oversized dimensions of safety devices. Beside the implications on cost, space and helium leakage, oversized safety valves often lead



to unstable operation during discharge with reduced relief flow capacity due to the so-called *pumping* or *chattering* of the safety valve.

In order to obtain a better understanding of the dynamic behavior, an analytic approach based on theoretical considerations and differential equation modeling of all time-dependent sub-processes was presented in [12]. The few simplifying assumptions in the model will be validated and extended with scaling parameters from experiments. Therefore, the cryogenic safety test facility PICARD, which stands for **P**ressure **I**ncrease in **C**ryostats and **A**nalysis of **R**elief **D**evelopments, has been designed, constructed and commissioned at the Karlsruhe Institute of Technology (KIT) [13].

The Kryolize<sup>®</sup> project, funded by CERN's Knowledge Transfer Group, was established to initiate an R&D collaboration with KIT for the experiments at PICARD. The results of the venting experiments will be included in the CERN Kryolize<sup>®</sup> software, a reference calculation program for the sizing of safety relief devices. [14]

This paper starts with a short overview of the PICARD test facility. In the main section, the commissioning and the general performance of PICARD at liquid helium temperatures is presented, before the results of the first venting experiments with focus on the helium pressure increase and the implications on the safety concept are discussed. In addition, a short outlook on further experiments planned in the course of the R&D collaboration between KIT and CERN is given.

## 2. PICARD test setup

The PICARD inner pressure vessel has a height of 900 mm, a cryogenic liquid volume of 100 L and a nominal design pressure of 16 bar(g). The maximum measurable helium relief flow rate through safety relief devices is up to 4 kg/s, which allows the systematic investigation of hazardous incidents in cryostats under realistic conditions, so called reasonably foreseeable events. A simplified CAD drawing and the piping and instrumentation diagram (P&ID) of PICARD is shown in figure 1. The test facility is equipped with a total of 31 sensors, including 18 cryogenic temperature sensors (TVO) inside the inner cryogenic vessel, at the surfaces of the inner vessel and the radiation shield, as well as inside the quench gas line. The TVO sensors inside the cryogenic vessel are located at 30 mm (TI14), 470 mm (TI15, TI13 and TI18) and 770 mm (TI12) measured from the bottom of the vessel. The data acquisition system has a maximum sampling rate of more than 1000 Hz. More detailed information on the setup of PICARD is given in [13].

Safety experiments in PICARD are triggered by venting gas at ambient temperature through an orifice into the insulation space of the cryostat, as can be seen in figure 1. The inflowing warm gas freezes out on the cold surface of the inner cryogenic vessel, causing a heat flux that is transferred to the cryogenic fluid. Both the temperature and the pressure of the cryogenic fluid increase until the set pressure is reached and the cryogenic fluid is released through an opening safety relief device.

Air humidity<sup>1</sup> that condenses and freezes out inside the vacuum space has to be removed completely from the system before vacuum can be pumped again, since water would damage the turbomolecular pump. Especially after venting experiments with multilayer insulation (MLI) applied to the inner vessel of the cryostat, the removal of moisture becomes challenging. Therefore, venting the insulating vacuum with gaseous nitrogen from a large buffer vessel with a volume of 400 l and a design pressure of 10 bar(g) is planned for experiments where MLI is applied.

<sup>1</sup> A considerable amount of water is introduced to the vacuum space during venting experiments with atmospheric air: Ambient air at KIT has an annual average relative humidity of about 75 % according to data from the DWD Climate Data Center (CDC) [15]. The relative humidity in the close surrounding of PICARD is measured with a combined humidity-temperature probe labeled MI31/TI31 in figure 1(b).

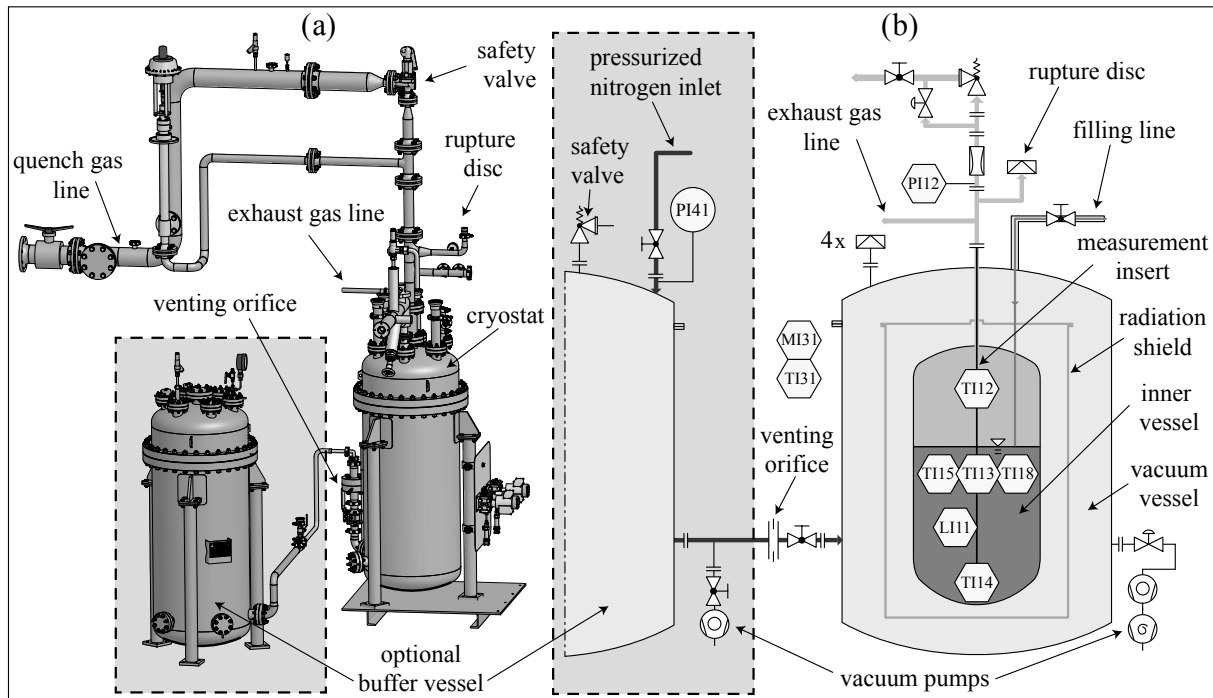


**Figure 1.** Simplified (a) CAD drawing and (b) P&ID of the PICARD test facility. As an addition to the test setup presented in [13], a buffer vessel highlighted in the gray boxes can be flanged to the venting orifice for venting experiments with gaseous nitrogen.

### 3. Commissioning

During the cooldown and filling process of the PICARD cryostat, an overpressure of 100 to 150 mbar was applied to the dewar vessel, transferring liquid helium through the filling line into the inner vessel of PICARD. Figure 2(a) shows the helium temperature over time from the start of the cooldown process at different heights inside the PICARD inner vessel. As seen in figure 1(b), the TVO sensors TI12, TI13 and TI14 are attached to the measurement insert inside the PICARD inner vessel at the top, middle and bottom, respectively.

In figure 2(b), the temperature profiles as shown in figure 2(a) are enlarged and complemented by the liquid level for the filling process that starts about 45 min after the start of the cooldown process. Due to the construction of the measurement insert, the helium liquid level  $a_{\text{LHe}}$  can only be measured with the superconducting liquid level sensor LI11 from a height of about  $a_{\text{LHe},0} = 3.5$  cm above the bottom of the PICARD inner vessel. The liquid level  $a_{\text{LHe,real}}$  shown in figure 2(b) was therefore calculated by

$$a_{\text{LHe,real}} = a_{\text{LHe,measured}} + a_{\text{LHe},0} \quad (1)$$

The helium pressure was measured with the pressure sensor PI12 to 0.1 bar(g) during the cooldown and filling process. The measured temperatures reached the corresponding boiling temperature of  $T_{\text{b,He}} = 4.3$  K once the temperature sensors were covered with liquid. Since the position of the temperature sensors inside the PICARD inner vessel is known, the filling level measurement with LI11 could be verified. Being fixed to the measurement insert at a height of 2.2 cm from the bottom of the inner vessel and below the range of LI11, the temperature sensor TI14 reached  $T_{\text{b,He}}$  after about 48 min. This corresponds very well with the extrapolated liquid level curve (dashed line). The TVO temperature sensor TI13, which is fixed at the

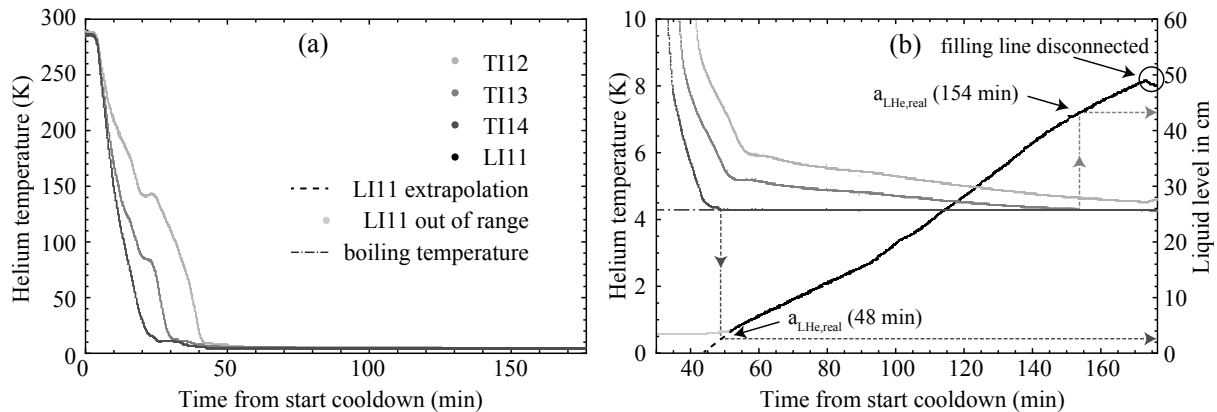


**Figure 2.** (a) Temperature profile and (b) enlarged temperature profile and real helium liquid level during the cooldown and filling process of the PICARD test facility. The position of the sensors inside the PICARD cryostat is given in figure 1(b).

middle of the inner vessel, reached  $T_{b,He}$  after about 154 min. This is also consistent with  $a_{LHe,real}(154 \text{ min}) = 43.5 \text{ cm}$ .

In total, it took about 173 min to cool down and fill the PICARD cryostat to a liquid level of 49 cm, which corresponds to about 60 l of liquid helium. During this time, 183 l of liquid helium were transferred from the dewar vessel to the PICARD cryostat and the inner vessel temperature decreased at a rate of up to 12 K/min. The measured vacuum pressure decreased from  $3.8 \cdot 10^{-6} \text{ mbar}$  in the beginning to  $5.7 \cdot 10^{-7} \text{ mbar}$  at the end of the filling process due to cryopumping effects. In the last three minutes of the data logging, the filling line was disconnected, resulting in the liquid level decrease and temperature increase visible in figure 2(b).

During idle time, the liquid level decreased with a rate of 3.2 mm/min. Thus, the evaporating helium mass flow rate  $\dot{m}_v$  could be calculated from the measured change in liquid volume  $\Delta V_{LHe}$  over the time period  $\Delta \tau$  and the helium density  $\rho_{liq}$  calculated from the measured boiling temperature of  $T_{b,He} = 4.3 \text{ K}$  using [16]. With the helium enthalpy of evaporation  $\Delta h_v$ , the heat input  $\dot{Q}$  during idle time was calculated by

$$\dot{Q} = \dot{m}_v \cdot \Delta h_v = \frac{\Delta V_{LHe}}{\Delta \tau} \cdot \rho_{liq} \cdot \Delta h_v \quad (2)$$

to  $\dot{Q} = 17 \text{ W}$ . Considering that the PICARD cryostat was not superinsulated with MLI, but only vacuum insulated with an aluminum radiation shield, this is a sufficiently good performance.

#### 4. Results of first venting experiments

Figure 3 shows the helium temperature and pressure increase over time from the start of the venting process of the first two experiments conducted with the settings listed in table 1. For these conditions, the safety valve of size DN25 was slightly *oversized* by about 25 % to 30 %, if one considers common design rules [3, 5, 7]. However, safety valves are only available in a grid of nominal sizes (DN20, DN25, DN32 etc.) with diameter increments of about 27 % [17]. In addition, incidents with heat loads and relief flow rates below the maximum design case are always possible and safety systems must be able to cope with such situations.

For both MP1 on the left and MP2 on the right of figure 3, the graphs are divided into three sectors. In sector I, the helium temperature and pressure increase isochorically in the closed inner vessel. The unstable operation of the safety valve is shown in sector II: During the repeated

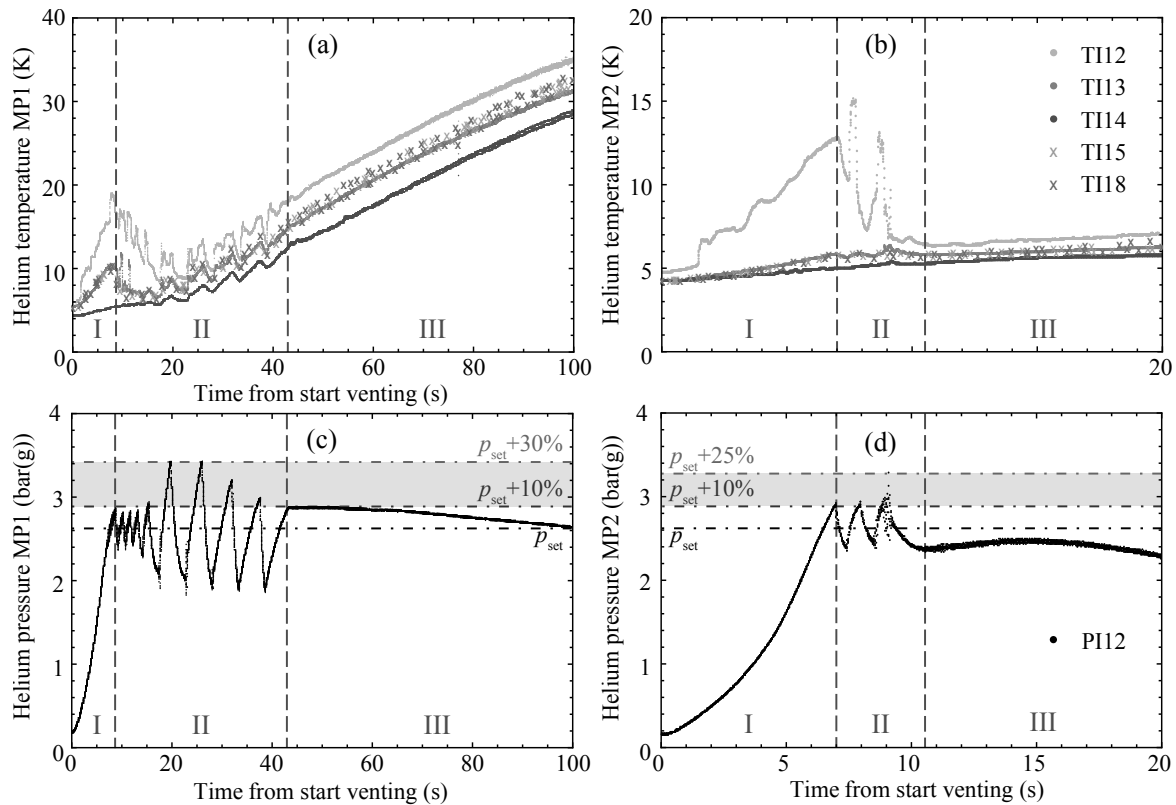


**Figure 3.** Helium temperature and pressure increase in the PICARD inner vessel during venting of the insulating vacuum with (a, c) gaseous nitrogen (MP1) and (b, d) atmospheric air (MP2). In sector I, the inner vessel is closed, the processes are isochoric. Sector II shows the unstable operation of the safety valve, before the helium pressure stably decreases in sector III.

**Table 1.** Settings of the conducted venting experiments number MP1 and MP2.

MP	Insulation	Venting fluid	Orifice diameter	Initial filling level	Cryogenic fluid	Set relief pressure	Sampling rate
1	Vacuum	Nitrogen	12.5 mm	28 %	Helium	2.6 bar(g)	150 Hz
2	Vacuum	Air	12.5 mm	53 %	Helium	2.6 bar(g)	150 Hz

opening and closing of the safety valve (*pumping*), both the helium pressure and temperature are subject to fluctuations. In sector III, the pressure inside the inner vessel decreases as helium is slowly released through the safety valve (*simmering*).

*Pumping* or *chattering* occurs when the inlet pressure drops quickly below the closing pressure of the safety valve during discharge. Causes for unstable operation can be large pressure drops in the inlet piping and oversizing of the safety valve [1, 2]. Resulting from good engineering practice, common design codes [7, 18] generally limit the pressure drop in the inlet piping to 3 % of the difference between the set pressure and the back pressure. However, higher pressure drops might be necessary and tolerable for cryogenic applications in order to reduce heat input to the system [1, 2]. In MP1 and MP2, the pressure losses were conservatively estimated to 4.7 %.

Since MP1 was conducted with gaseous nitrogen as venting fluid, the buffer vessel shown in figure 1 was attached to the venting orifice for this experiment. In order to protect the rupture discs of the PICARD vacuum vessel set to 0.5 bar(g), gaseous nitrogen was supplied in the buffer vessel with an overpressure of 1 bar(g) and constantly refilled during venting until ambient pressure was reached in the vacuum space. However, the cryopumping of the helium vessel was more effective than expected and the pressure in the buffer vessel stagnated at 300 mbar(a) because not enough nitrogen could be refilled from the 200 bar(g) nitrogen cylinder. After about 200 s, the temperature of the inner vessel wall exceeded the melting point of nitrogen and the vacuum pressure increased to 1000 mbar(a). Therefore, the processes shown in figure 3(a) and (c) are considerably slower than in figure 3(b) and (d), and the safety valve pumps more frequently and for a longer period during unstable operation in sector II. The results of MP1 illustrate that a smaller incident (compared to MP2) can be more problematic with regard to the valve operation and the maximum vessel pressure.

The temperature increase inside the inner vessel is shown in figure 3(a) and figure 3(b). In both the graphs, a stratification between the three temperature sensors TI12, TI13 and TI14 at the top, middle and bottom can be observed, while the horizontal temperature gradients measured by TI15, TI13 and TI18 are small.

The helium pressure increase measured by the transmitter PI12 is shown in figure 3(c) and figure 3(d). The set pressure is defined as the pressure at which the pressure relief device opens under predetermined conditions [3, 5]. However, the certification of such set pressure may vary depending on the type of pressure relief device and on the test procedure used. For instance, four different test procedures to qualify the set pressure are listed in [1]: “initial audible discharge”, “pop action” (for full-lift safety valves), “start to leak pressure” and “bubble test”. Measurements at KIT showed the difference between the set pressure according to the “bubble test” and “initial audible discharge” of about 20...25% with regard to the latter value. For both experiments MP1 and MP2 at PICARD, the safety valve was set to  $p_{\text{set}} = 2.6$  bar(g) at “initial audible discharge”.

According to the standards [3, 5, 7], the safety valve must open completely within  $p_{\text{set}} + 10\%$ , i.e. at  $p \leq 2.9$  bar(g), which was the case in MP1 and MP2. However, the pressure increased up to  $p_{\text{set}} + 25\%$  in MP2, and even up to  $p_{\text{set}} + 30\%$  in MP1<sup>2</sup>. Such an overpressure could have triggered the bursting of the rupture disc in a staged cryostat protection system, where the margin<sup>3</sup> between the set pressures had been too small. Consequences might be large helium losses and the possible contamination of the open system with air moisture. For systems without an additional protection level, such overpressures could lead to plastic deformation.

The safety valve in PICARD is mounted at 1.3 m above the cryostat at ambient temperature, i.e. it is not in contact with cold gas before the initial opening, but cools down during discharge. Therefore, the temperature decrease of the safety valve causing an increased stiffness of the spring may explain the further pressure increase after 20 s in MP1 and after 9 s in MP2. Another explanation for the increasing pressure during discharge could be the occurrence of two-phase flow, which reduces the discharge capacity of safety relief devices [1, 2]. The effects will be studied in more detail in the future.

## 5. Conclusions and Outlook

The PICARD test facility has successfully been commissioned at liquid helium temperatures. The fast cooldown and filling processes in combination with the low heat input during idle time allow the cooldown and filling process, as well as a venting experiment to be completed within

<sup>2</sup> Since the bursting pressure of the rupture disc as ultimate pressure protection level was set to the design pressure of  $p_S = 16$  bar(g), the overpressure was without consequence for the PICARD test facility.

<sup>3</sup> A recommended margin value is 30% to fulfill the tolerances of +10% for the safety valve and  $\pm 10\%$  for the rupture disc [1, 2].

one day. First venting experiments with gaseous nitrogen and atmospheric air as venting fluids have been conducted.

The first results already show the significance of the experiments, as significant overpressures with regard to the set pressure were observed during unstable operation of the safety valve. Similar observations were made in yet unpublished experiments at CERN. Therefore, more experiments with different safety valves and additional instrumentation will be conducted in order to detect the causes and find possible solutions.

Beside the investigation of safety valve characteristics in the temperature range of 4 to 300 K, further experiments at PICARD will focus on maximum foreseeable events with larger heat loads, realized by larger venting orifices in combination with higher set relief pressures. Additionally, the influence of MLI and relief pressures close to the critical point of helium will be investigated in the frame of the R&D collaboration between KIT and CERN.

### Acknowledgments

We would like to acknowledge the support from the Karlsruhe School of Elementary Particle and Astroparticle Physics: Science and Technology (KSETA). We would also like to acknowledge the support from the CERN Knowledge Transfer Group and the KIT Legal Department in the process of finalizing the R&D collaboration agreement.

### References

- [1] DIN SPEC 4683 2015 Cryostats for liquefied helium - Safety devices for protection against excessive pressure
- [2] Grohmann S and Süßer M 2014 *AIP Conf. Proc.* **1573** 1581–85
- [3] DIN EN ISO 4126-1 2004 Safety devices for protection against excessive pressure - Part 1: Safety valves
- [4] DIN EN 13648-3 2003 Cryogenic vessels - Safety devices for protection against excessive pressure - Part 3: Determination of required discharge - Capacity and sizing
- [5] API 520-1 2000 Sizing, selection, and installation of pressure-relieving devices in refineries - Part 1: Sizing and selection
- [6] AD 2000-Merkblatt A 1 2006 Sicherheitseinrichtungen gegen Drucküberschreitung - Berstsicherungen
- [7] AD 2000-Merkblatt A 2 2012 Sicherheitseinrichtungen gegen Drucküberschreitung - Sicherheitsventile
- [8] Varghese A P and Zhang B X 1991 *Adv. Cryog. Eng.* **37** 1487–93
- [9] Lehmann W and Zahn G 1978 *Proc. Int. Cryog. Eng. Conf.* **7** 569–579
- [10] Harrison S M 2002 *IEEE T. Appl. Superconductivity* **12** 1343–46
- [11] Cavallari G, Gorin I, Güsewell D and Stierlin R 1989 *Proc. 4<sup>th</sup> Workshop on RF Superconductivity* **1** 781–803
- [12] Heidt C, Grohmann S and Süßer M 2014 *AIP Conf. Proc.* **1573** 1574–80
- [13] Heidt C, Schön H, Stamm M and Grohmann S 2015 *IOP Conf. Ser.: Mater. Sci. Eng.* **101** 012161
- [14] Henriques A 2015 KT Fund Application for Kryolize Project *CERN EDMS N. 1554181*
- [15] DWD Climate Data Center (CDC) 2016 Tageswerte der Station 10731 Rheinstetten URL <http://www.dwd.de/DE/leistungen/klimadatendeutschland/klimadatendeutschland.html#> [retrieved 2016/02/29]
- [16] Lemmon E W, Huber M L and McLinden M O 2010 *NIST Standard Reference Database 23: Reference Fluid Thermodynamic and Transport Properties - REFPROP* 9<sup>th</sup> ed
- [17] LESER GmbH & Co KG 2012 *High Performance Catalog 1* May 2012/2.000 ed
- [18] ISO 4126-9 2008 Safety devices for protection against excessive pressure - Part 9: Application and installation of safety devices excluding stand-alone bursting disc safety devices